

# On-Line Trajectory Optimization Including Moving Threats and Targets

Shannon Twigg<sup>\*</sup>, Anthony Calise<sup>†</sup> and Eric Johnson<sup>‡</sup>

*School of Aerospace Engineering, Georgia Institute of Technology, Atlanta, GA 30332-0150*

## Abstract

Different methods of optimizing terrain following trajectories have been investigated as an extension of earlier reduced order formulations. This paper incorporates wind, moving threats -- such as other aircraft to be avoided -- and a moving target -- such as a rendezvous situation -- into the basic constant velocity formulation. Consequently, this will allow a more realistic model to be simulated. In addition, changing information, such as a threat appearing during flight, are considered. The reduced order formulation results in a system of four differential equations with two unknown initial conditions. The solution is found with the use of a genetic algorithm in conjunction with a conjugate-gradient numerical search method.

## I. Introduction

High-flying unmanned reconnaissance and surveillance systems are now being used extensively in the United States military. Current development programs are producing demonstrations of next-generation unmanned flight systems that are designed to perform combat missions. Their use in first-strike combat operations will dictate operations in densely cluttered environments that include unknown obstacles and threats, and will require the use of terrain for masking. The demand for autonomy of operations in such environments dictates the need for rapid on-board trajectory optimization capability.

In the early 1990s, P. K. Menon and Eulgon Kim researched methods of optimal trajectory path planning for terrain following and terrain masking flight. This research produced a reduced order formulation based on a constant velocity approach.<sup>1,2</sup> This paper expands on the work done by Menon and Kim. Two formulations are presented: one using local tangent plane equations of motion and one using simplified equations of motion. In addition, the effects of wind, moving threats and a moving target are added. The moving threat could consist of an object, such as an aircraft, that should be avoided during flight. The moving target would be a moving destination, or a rendezvous problem. Also, the addition of a pop-up threat is examined.

## II. Optimal Trajectory Formulations

The effects of wind as well as having a moving target and moving threat are added to the basic problem formulated in References 1 and 2. This will be demonstrated in two different formulations -- one using the local tangent plane equations of motion and one utilizing simplified equations of motion. Figure 1 depicts a sample terrain profile with the X-Y-H coordinate system and a local x<sub>1</sub>-y<sub>1</sub>-z<sub>1</sub> coordinate system. The moving local coordinate system has its origin on the terrain surface at a current x, y position with the x<sub>1</sub>-y<sub>1</sub> plane being the tangent plane. The local tangent plane formulation incorporates the constraint that the vehicle flies tangentially to the local terrain directly into the equations of motion and can be written as

$$\dot{x} = \frac{V \cos \gamma}{A_1} + \frac{V f_x f_y \sin \gamma}{A_1 A_2} + u(x, y) \quad (1)$$

$$\dot{y} = \frac{-V A_1 \sin \gamma}{A_2} + v(x, y) \quad (2)$$

---

<sup>\*</sup>AIAA member, Graduate Research Assistant, Georgia Institute of Technology, Atlanta, Georgia

<sup>†</sup>AIAA Fellow, Professor, Georgia Institute of Technology, Atlanta, Georgia

<sup>‡</sup>AIAA member, Assistant Professor, Georgia Institute of Technology, Atlanta, Georgia

The simplified equations of motion are an approximation written in the local level frame and neglect the effects of the terrain slope in the position kinematics.

$$\dot{x} = V \cos \gamma + u(x, y) \quad (3)$$

$$\dot{y} = V \sin \gamma + v(x, y) \quad (4)$$

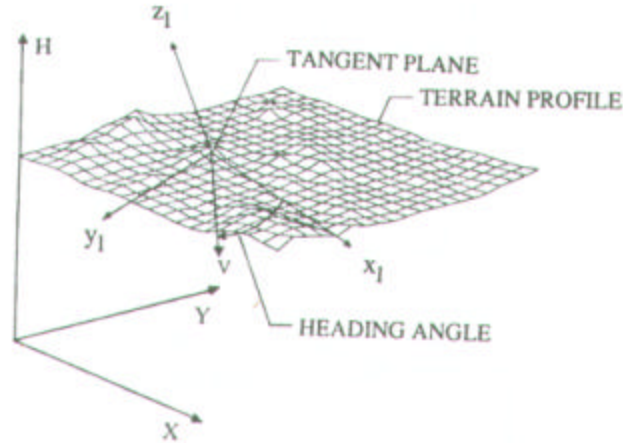


Figure 1: Relationship Between Inertial Frame and Local Tangent Plane

#### A. Local Tangent Plane Equations of Motion

In this formulation, the equations of motion can be seen above in equations (1) and (2). These equations embody the constraint that at all times the vehicle flies tangentially to the local terrain. Here,  $x$  and  $y$  are the north and east components, respectively.  $V$  is the total aircraft velocity while  $u$  and  $v$  are the wind velocities in the  $x$  and  $y$ -directions, respectively. The heading of the vehicle is represented by  $\gamma$  -- the heading angle measured with respect to the local tangent plane. Also,  $f_x$  and  $f_y$  are the partial derivatives of the terrain profile.  $A_1$  and  $A_2$  are given by

$$A_1 = \sqrt{1 + f_x^2} \quad (5)$$

$$A_2 = \sqrt{1 + f_x^2 + f_y^2} \quad (6)$$

The cost function for this problem can be seen in the following equation.

$$J = \int_0^t [(1 - K) + Kg(x, y, t)] dt \quad (7)$$

In this equation, the combined threat and terrain function,  $g(x, y, t)$ , is given as a function of time as well as the position and can be defined as follows.

$$g(x, y, t) = f(x, y) + f_T(x, y, t) \quad (8)$$

Here,  $f(x, y)$  is the function for the terrain profile and  $f_T(x, y, t)$  is the function denoting the moving threat. The weighting parameter,  $K$ , can vary between 0 and 1 and determines the relative importance of time and terrain masking/threat avoidance used in the optimization. When  $K = 0$ , the equations are optimized with respect to time.

When  $K$  is set to 1, the path is optimized with respect to the threats and the terrain. The Hamiltonian equation can then be given as

$$H = A_4 + I_x \left[ \frac{V \cos \mathbf{y}}{A_1} + \frac{V f_x f_y \sin \mathbf{y}}{A_1 A_2} + u \right] + I_y \left[ \frac{-V A_1 \sin \mathbf{y}}{A_2} + v \right] \quad (9)$$

In this expression,  $I_x$  and  $I_y$  are the costate equations and the coefficient  $A_4$  can be seen in the following equation.

$$A_4 = 1 - K + Kg(x, y, t) \quad (10)$$

The moving threat and target equations of motion are:

$$\dot{x}_T = V_T \cos \mathbf{y}_T \quad (11)$$

$$\dot{y}_T = V_T \sin \mathbf{y}_T$$

$$\dot{x}_{Tg} = V_{Tg} \cos \mathbf{y}_{Tg} \quad (12)$$

$$\dot{y}_{Tg} = V_{Tg} \sin \mathbf{y}_{Tg}$$

In each expression, it is assumed that the respective velocity and heading angle are known at all times. The moving target then results in a new boundary condition.

$$\Psi(t_f) = \left[ \begin{array}{c} x(t) - x_{Tg}(t) \\ y(t) - y_{Tg}(t) \end{array} \right]_{t=t_f} \quad (13)$$

In this expression, it can be seen that  $\Psi(t_f)$  has an explicit dependence on the final time as a consequence of the fact that the target coordinates are assumed to satisfy equation (12). Therefore, for a free final time, the Hamiltonian equation satisfies

$$H(t_f) = -\mathbf{I}^T \left[ \frac{\partial \Psi}{\partial t} \right]_{t=t_f} = V_{Tg} \left[ I_x \cos \mathbf{y}_{Tg} + I_y \sin \mathbf{y}_{Tg} \right]_{t=t_f} \quad (14)$$

Due to the moving threat, the Hamiltonian equation, (9), is explicitly dependent on time. Given this, the optimality condition for a solution along an extremal arc shows that

$$\dot{H} = \frac{\partial H}{\partial t} = Kg_t \quad (15)$$

where  $g_t$  denotes the partial derivative of the penalty function with respect to time. Assuming that the threat is constant when expressed in a coordinate system that is attached to the moving threat, then

$$g(x, y, t) = g[x - x_T(t), y - y_T(t)] \quad (16)$$

with the threat coordinates satisfying (11). Thus

$$\dot{H} = -KV_T (g_x \cos \mathbf{y}_T + g_y \sin \mathbf{y}_T) \quad (17)$$

Because the final time is free, the boundary condition for this expression is defined in (14).  
The optimality condition for this problem is defined as

$$H_y = 0 \quad (18)$$

Evaluating this expression results in the following relationship

$$I_y = I_x \left[ \frac{V f_x f_y \cos \mathbf{y}}{A_1 A_2} - \frac{V \sin \mathbf{y}}{A_1} \right] \frac{A_2}{V A_1 \cos \mathbf{y}} \quad (19)$$

Equation (19) can then be substituted into the Hamiltonian equation, (7), to determine equations defining the two costates,  $\lambda_x$  and  $\lambda_y$  as follows.

$$I_x = \frac{-(A_4 - H) A_1^2 \cos \mathbf{y}}{Den} \quad (20)$$

$$I_y = \frac{(A_4 - H) A_2 \sin \mathbf{y} - (A_4 - H) f_x f_y \cos \mathbf{y}}{Den} \quad (21)$$

where

$$Den = V A_1 + A_1^2 u \cos \mathbf{y} + f_x f_y v \cos \mathbf{y} - A_2 v \sin \mathbf{y} \quad (22)$$

These new expressions for the costates can then be inserted into (14) to result in a new boundary condition for the Hamiltonian at the final time.

$$H(t_f) = \left[ \frac{V_{T_g} A_4 (A_1^2 \cos \mathbf{y} \cos \mathbf{y}_{T_g} + f_x f_y \cos \mathbf{y} \sin \mathbf{y}_{T_g} - A_2 \sin \mathbf{y} \sin \mathbf{y}_{T_g})}{V_{T_g} (A_1^2 \cos \mathbf{y} \cos \mathbf{y}_{T_g} + f_x f_y \cos \mathbf{y} \sin \mathbf{y}_{T_g} - A_2 \sin \mathbf{y} \sin \mathbf{y}_{T_g}) - Den} \right]_{t=t_f} \quad (23)$$

Differential equations for the costates can be found using

$$\begin{aligned} \dot{I}_x &= -H_x \\ \dot{I}_y &= -H_y \end{aligned} \quad (24)$$

This yields

$$\dot{I}_x = -K g_x - I_x \left[ \frac{D_2 \cos \mathbf{y} + D_3 \sin \mathbf{y} + D_1 u_x}{D_1} \right] - I_y \left[ \frac{D_4 \sin \mathbf{y} + D_1 v_x}{D_1} \right] \quad (25)$$

$$\dot{I}_y = -K g_y - I_x \left[ \frac{D_5 \cos \mathbf{y} + D_6 \sin \mathbf{y} + D_1 u_y}{D_1} \right] - I_y \left[ \frac{D_7 \sin \mathbf{y} + D_1 v_y}{D_1} \right] \quad (26)$$

where

$$D_1 = A_1^3 A_2^3 \quad (27)$$

$$D_2 = -V f_x f_{xx} A_2^3 \quad (28)$$

$$D_3 = V A_1^2 A_2^2 B_2 - V A_2^2 f_x^2 f_y f_{xx} - V A_1^2 B_1 f_x f_y \quad (29)$$

$$D_4 = VA_1^4 B_1 - VA_1^2 A_2^2 f_x f_{xx} \quad (20)$$

$$D_5 = -V f_x f_{xy} A_2^3 \quad (31)$$

$$D_6 = VA_1^2 A_2^2 B_3 - VA_2^2 f_x^2 f_y f_{xy} - VA_1^2 B_4 f_x f_y \quad (32)$$

$$D_7 = VA_1^4 B_4 - VA_1^2 A_2^2 f_x f_{xy} \quad (33)$$

$$B_1 = f_x f_{xx} + f_y f_{xy} \quad (34)$$

$$B_2 = f_x f_{xy} + f_y f_{xx} \quad (35)$$

$$B_3 = f_x f_{yy} + f_y f_{xy} \quad (36)$$

$$B_4 = f_x f_{xy} + f_y f_{yy} \quad (37)$$

Next, the time derivative of either equation (20) or (21) is taken and set equal to its counterpart in equation (25) or (26). The resulting expression is

$$\dot{\mathbf{y}} = \frac{T_1 + T_2 u + T_3 v + T_4 u_x + T_5 u_y + T_6 v_x + T_7 v_y}{T_8} \quad (38)$$

where

$$T_1 = -KVS_1 + V(A_4 - H)S_2 \quad (39)$$

$$T_2 = -KS_3 + (A_4 - H)S_4 \quad (40)$$

$$T_3 = KS_5 + (A_4 - H)S_6 \quad (41)$$

$$T_4 = (A_4 - H)S_7 \quad (42)$$

$$T_5 = (A_4 - H)S_8 \quad (43)$$

$$T_6 = (A_4 - H)S_9 \quad (44)$$

$$T_7 = (A_4 - H)S_{10} \quad (45)$$

$$T_8 = (A_4 - H)A_1^3 A_2^2 \quad (46)$$

$$S_1 = A_1^2 A_2 [A_2 g_x \sin \mathbf{y} + (g_y + f_x^2 g_y - g_x f_x f_y) \cos \mathbf{y}] \quad (47)$$

$$S_2 = (f_x f_y^2 f_{xx} - A_1^2 f_y f_{xy}) \sin \mathbf{y} + A_2 f_y f_{xx} \cos \mathbf{y} \quad (48)$$

$$S_3 = A_1^3 A_2 [A_2 g_x \sin \mathbf{y} + (g_y + f_x^2 g_y - g_x f_x f_y) \cos \mathbf{y}] \cos \mathbf{y} \quad (49)$$

$$S_4 = A_1 A_2 (A_1^2 f_x f_{xy} - f_x^2 f_y f_{xx} + f_y f_{xx}) \cos^2 \mathbf{y} + A_1 (A_1^2 f_x f_{xx} - A_1^2 f_y f_{xy} + 2f_x f_y^2 f_{xx}) \sin \mathbf{y} \cos \mathbf{y} \quad (50)$$

$$S_5 = A_1 A_2^2 (A_1^2 g_y - 2g_x f_x f_y) \sin \mathbf{y} \cos \mathbf{y} + A_1 A_2^3 g_x \sin^2 \mathbf{y} + A_1 A_2 (g_x f_x^2 f_y^2 - A_1^2 f_x g_y f_y) \cos^2 \mathbf{y} \quad (51)$$

$$S_6 = A_1 A_2 (f_y f_{xy} - f_x^2 f_y f_{xy} + A_1^2 f_x f_{yy}) \cos^2 \mathbf{y} + A_1 (2f_x f_y^2 f_{xy} + A_1^2 f_x f_{xy} - A_1^2 f_y f_{yy}) \sin \mathbf{y} \cos \mathbf{y} \quad (52)$$

$$S_7 = A_1^3 A_2 (A_2 \sin \mathbf{y} - f_x f_y \cos \mathbf{y}) \cos \mathbf{y} \quad (53)$$

$$S_8 = A_1^5 A_2 \cos^2 \mathbf{y} \quad (54)$$

$$S_9 = A_1 A_2^2 (2f_x f_y \sin \mathbf{y} \cos \mathbf{y} - A_2) + A_1 A_2 (A_2^2 - f_x^2 f_y^2) \cos^2 \mathbf{y} \quad (55)$$

$$S_{10} = A_1^3 A_2 (f_x f_y \cos \mathbf{y} - A_2 \sin \mathbf{y}) \cos \mathbf{y} \quad (56)$$

This solution consists of four differential equations,  $x$ ,  $y$ ,  $H$  and  $\mathbf{y}$ , and requires two initial conditions to be found for  $H$  and  $\mathbf{y}$ . The final value of the Hamiltonian is known, via equation (23). The solution is reached when the final values of the Hamiltonian and position are met and the cost is minimized. When there are no moving threats, the Hamiltonian is constant in value – so there are only three differential equations – and the final value is still known. When there is no moving target, the final value of the Hamiltonian is zero.

### B. Simplified Equations of Motion

The equations of motion used in the simplified formulation are stated above in equations (3) and (4) and are restated here

$$\begin{aligned} \dot{x} &= V \cos \mathbf{y} + u(x, y) \\ \dot{y} &= V \sin \mathbf{y} + v(x, y) \end{aligned}$$

These equations are written in the local level plane and neglect the effects of the terrain slope. The cost equation for this case is the same as earlier and can be found in equation (7). The corresponding Hamiltonian equation is therefore

$$H = A_4 + \mathbf{I}_x [V \cos \mathbf{y} + u] + \mathbf{I}_y [V \sin \mathbf{y} + v] \quad (59)$$

The equations governing the moving target and moving threat can be seen above in equations (11) through (12).

Evaluating the optimality condition stated in equation (18) for this formulation results in the expression

$$\mathbf{I}_y = \mathbf{I}_x \frac{\sin \mathbf{y}}{\cos \mathbf{y}} \quad (60)$$

Substituting this into the Hamiltonian equation results in the following costate equations

$$\mathbf{I}_x = \frac{-(A_4 - H) \cos \mathbf{y}}{V + u \cos \mathbf{y} + v \sin \mathbf{y}} \quad (61)$$

$$\mathbf{I}_y = \frac{-(A_4 - H) \sin \mathbf{y}}{V + u \cos \mathbf{y} + v \sin \mathbf{y}} \quad (62)$$

Therefore, the Hamiltonian evaluated at the final time will be

$$H(t_f) = \left[ \frac{V_{Tg} A_4 \cos(\mathbf{y} - \mathbf{y}_{Tg})}{V_{Tg} \cos(\mathbf{y} - \mathbf{y}_{Tg}) - (V + u \cos \mathbf{y} + v \sin \mathbf{y})} \right]_{t=t_f} \quad (63)$$

The costate differential equations can then be found to be

$$\dot{\mathbf{I}}_x = -H_x = -K g_x - \mathbf{I}_x u_x - \mathbf{I}_y v_x \quad (64)$$

$$\dot{\mathbf{I}}_y = -H_y = -K g_y - \mathbf{I}_x u_y - \mathbf{I}_y v_y \quad (65)$$

As before, the time derivative of (61) or (62) is found and equated to either (64) or (65). This expression can then be rearranged to result in the following heading differential equation.

$$\dot{\mathbf{y}} = \frac{R_1 + R_2u + R_3v + R_4(u_x - v_y) + R_5u_y + R_6v_x}{R_7} \quad (66)$$

with

$$R_1 = KV(g_y \cos \mathbf{y} - g_x \sin \mathbf{y}) \quad (67)$$

$$R_2 = K(g_y \cos \mathbf{y} - g_x \sin \mathbf{y}) \cos \mathbf{y} \quad (68)$$

$$R_3 = K(g_y \cos \mathbf{y} - g_x \sin \mathbf{y}) \sin \mathbf{y} \quad (69)$$

$$R_4 = (A_4 - H) \sin \mathbf{y} \cos \mathbf{y} \quad (70)$$

$$R_5 = -(A_4 - H) \cos^2 \mathbf{y} \quad (71)$$

$$R_6 = (A_4 - H) \sin^2 \mathbf{y} \quad (72)$$

$$R_7 = (A_4 - H) \quad (73)$$

Again, the inclusion of a moving target and moving threat results in a system of four differential equations with two initial parameters to be found.

### C. Solving the System of Equations

As stated earlier, the problem, in its most complex form having both a moving target and a moving threat, consists of four differential equations with two unknown initial conditions. The differential equations include the two describing the position as well as the Hamiltonian equation and the heading angle. The initial conditions for both the Hamiltonian and the heading angle are unknown. The problem is solved when the final positions equal the moving target final positions, the actual final Hamiltonian value matches its final condition -- from equations (23) and (63) -- and the cost is minimized.

To solve this problem, two numerical solving techniques were employed. First a genetic algorithm was used to find initial conditions that are close to the actual initial conditions needed. Next, these values are employed in a conjugate-gradient search method to find the actual desired initial conditions.

The genetic algorithm was accomplished by first creating a random population of ten chromosomes each consisting of nine digits -- the first five representing the initial Hamiltonian value and the last four determining the initial heading angle. Then, twenty more chromosomes were created by randomly mutating the original ten chromosomes. After the full population of thirty was created, each was tested in the routines to determine a cost. The cost,  $C$ , was valued through the equation

$$C = c_1 \cdot dist + c_2 \cdot J + c_3 \cdot err \quad (74)$$

Here,  $c_1$ ,  $c_2$  and  $c_3$  are weighting values,  $dist$  is the distance between the final position and the final target position,  $J$  is the cost of the run found from equation (7) and  $err$  is the difference between the actual and desired final Hamiltonian. The ten chromosomes with the lowest costs were then kept to begin the next generation. This process was repeated for thirty generations and the chromosome at the end with the lowest cost was used as the starting position of the conjugate search.

The conjugate search method is a form of a steepest descent search. First the gradient of the surface defined by the cost -- as seen in equation (74) -- at a test point is determined. The search direction is then defined as the direction having the steepest gradient. Various points are checked along this direction until a minimum is found. After the first step, this basic process is repeated; however, to determine the new search directions the gradient information from the previous run is included such that the new search directions are conjugate.<sup>6</sup>

### III. Numerical Results

#### A. Real Terrain Data

Real terrain data was acquired from the United States Geological Survey to incorporate into this model<sup>3</sup>. The data was found in tabular format relating the altitude to the locations longitude and latitude, with data points spaced approximately every 48 feet. This data was then converted to matrix form, from which it could then be used as  $f(x, y)$ . Because of the distance between the sampled altitude points in the matrix, the data was then smoothed to appear more continuous and to remove discontinuities in altitude. The gradients of this matrix, along both the x and y directions, were calculated numerically to form matrices representing  $f_x(x, y)$  and  $f_y(x, y)$ . The gradients of these two matrices yielded matrices for  $f_{xx}(x, y)$ ,  $f_{yy}(x, y)$  and  $f_{xy}(x, y)$ .

For this portion of the testing, it was decided to use a section of terrain near Columbus, Ohio. A profile of this terrain can be seen in Figure 2. In this graph, the x and y-axes depict the position coordinates, measured in feet, such that the x axis point north and the y axis points east. The altitude of the terrain is measured along the z-axis and is also given in feet. This plot depicts a square plot of land, with 10,000 feet to a side. The measurements along the x and y-axes are relative to a set origin for the terrain data collected; this plot is just one small portion of the database.

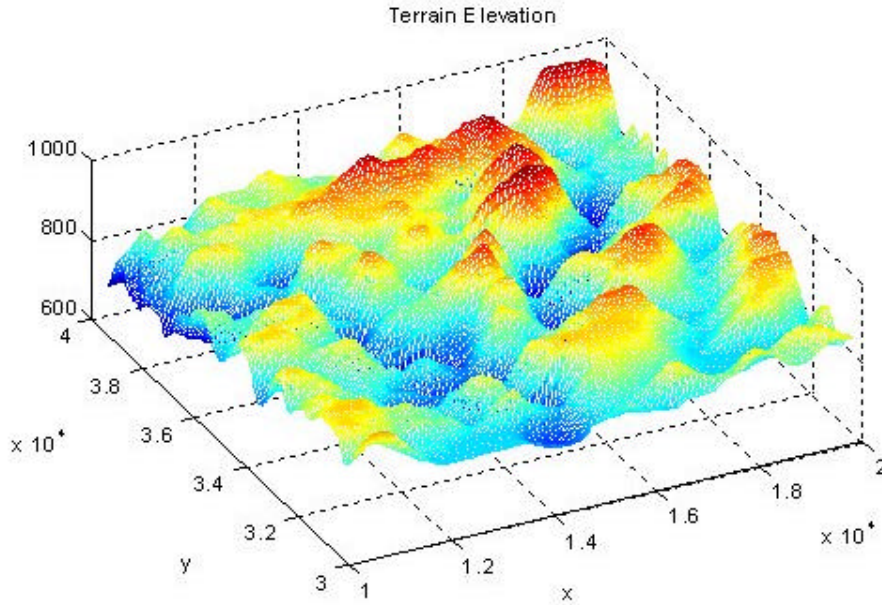


Figure 2: Terrain Plot of an Area Near Columbus Ohio

#### B. Wind Effects

Next, the effects of a wind blowing were investigated. For this, a mostly flat plane with a single hill was used, as shown in Figure 3. This terrain was formulated using the exponential function

$$f = Ae^{-r^2/b} \tag{75}$$

where  $A$  is the amplitude,  $b$  is a scaling factor to adjust the width and  $r$  is the distance from any position to the center of the threat.

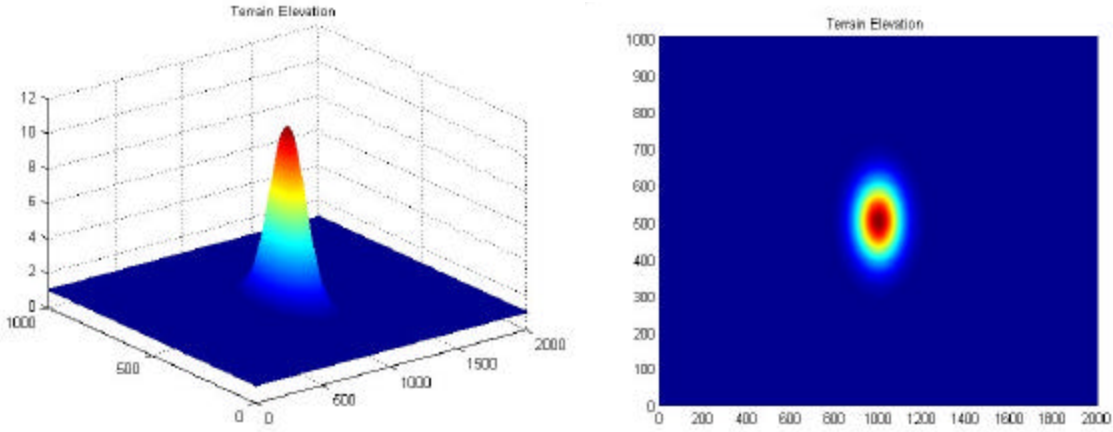


Figure 3: Terrain with threats formulated as an exponential function. On the right is an overhead view.

For these flights, the initial and final points are (500,1800) and (500,200). Therefore the hill is directly between the two endpoints. With  $K$  set to 1, the optimal path found will curve around the hill. Since this is a symmetric field, there are two possible optimal paths when there is no wind.

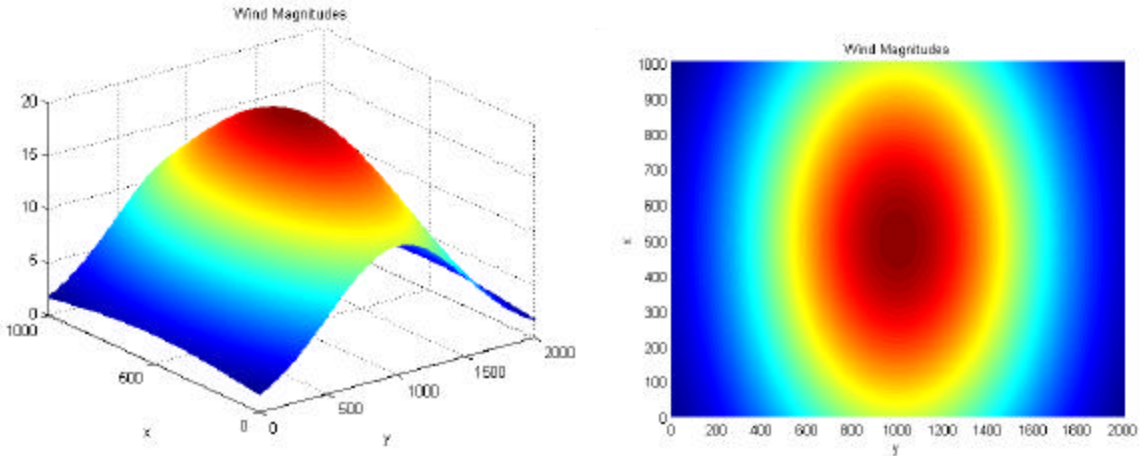


Figure 4: Wind magnitudes of a circulating pattern.

Here, a circulating wind pattern was introduced to the problem. In this case, the wind moved in a circular pattern centered at the top of the hill with a decreasing speed moving away from the hill. The magnitudes of the wind can be seen in Figure 4. This plot was generated using equation (75); however, in this case,  $A$  and  $b$  were set to 20 and 500000, respectively.

With the winds added, the optimal path is the option where the aircraft moves in the same direction as the circulating wind flow. Figure 5 shows the solutions found with the winds moving in a clockwise direction – on the left – and in a counterclockwise direction – on the right. In both cases, the local tangent plane equations of motion were utilized.

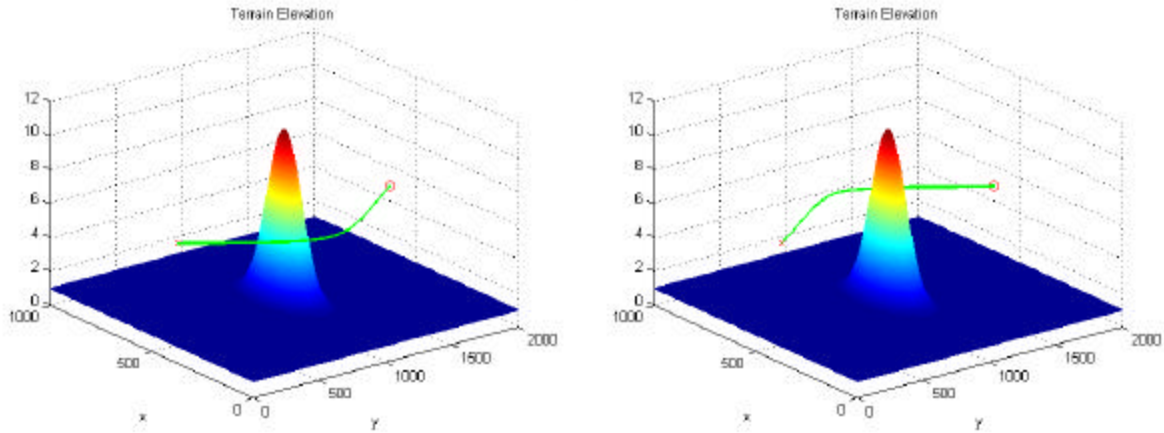


Figure 5: Optimal path from (500,1800) to (500,200). The figure on the left shows the optimal path with a clockwise wind while the figure on the right shows the optimal path with a counterclockwise path.

### C. Moving Target and Threats

The simple terrain depicted above in Figure 3 consisting of a flat plain with a single hill was used to test the moving threat and target. The initial position is again located at (500, 1800). The moving target begins at the point (900, 200) and travels south while the two threats begin at (600, 100) and (600, 400), respectively, and travel in a south-easterly direction.

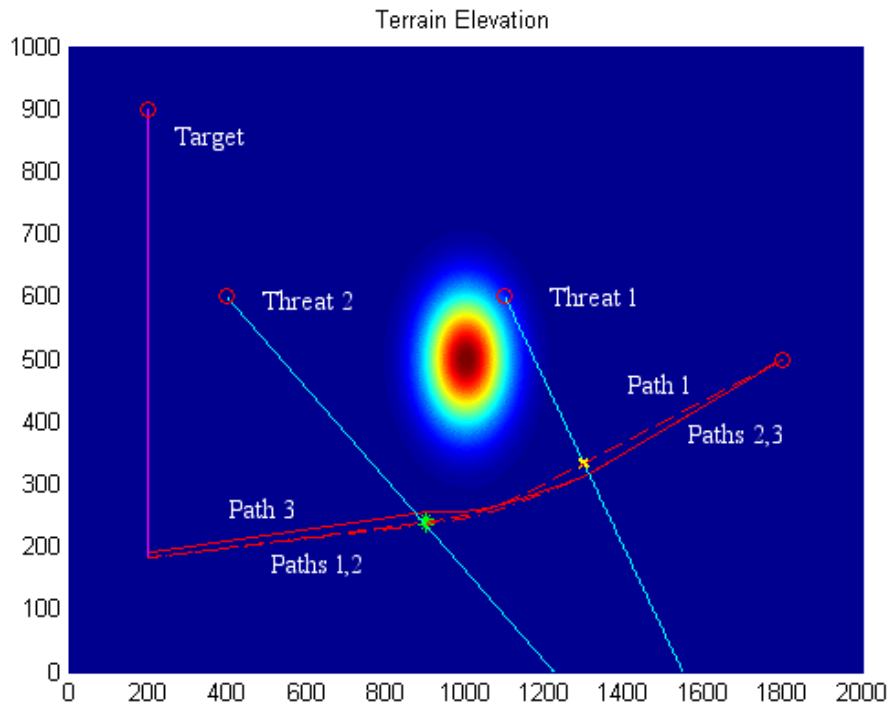


Figure 6: Paths Generated with Consideration of a Moving Target and Two Moving Threats Using Local Tangent Plane Equations of Motion

Figure 6 shows the three results using the local tangent plane equations of motion. The beginning position for each trajectory is marked with a red circle. The moving target is indicated with a purple line while the moving

threats are represented with blue lines. The first case -- Path 1 -- is using just a moving target, but no moving threats. This trajectory is depicted by the red dashed line. The yellow x marks the spot where Path 1 intersects Threat 1 at the same instant. Path 2 represents the trajectory when the moving target and the first moving threat are considered and is portrayed by a red dot-dash line. The green star shows the moment when the Path 2 and Threat 2 collide. The third path shows the trajectory when both the threats are considered and is illustrated by a solid red line. Next is the case with one moving threat that intersects the original trajectory determined. The final path results from the addition of a second threat.

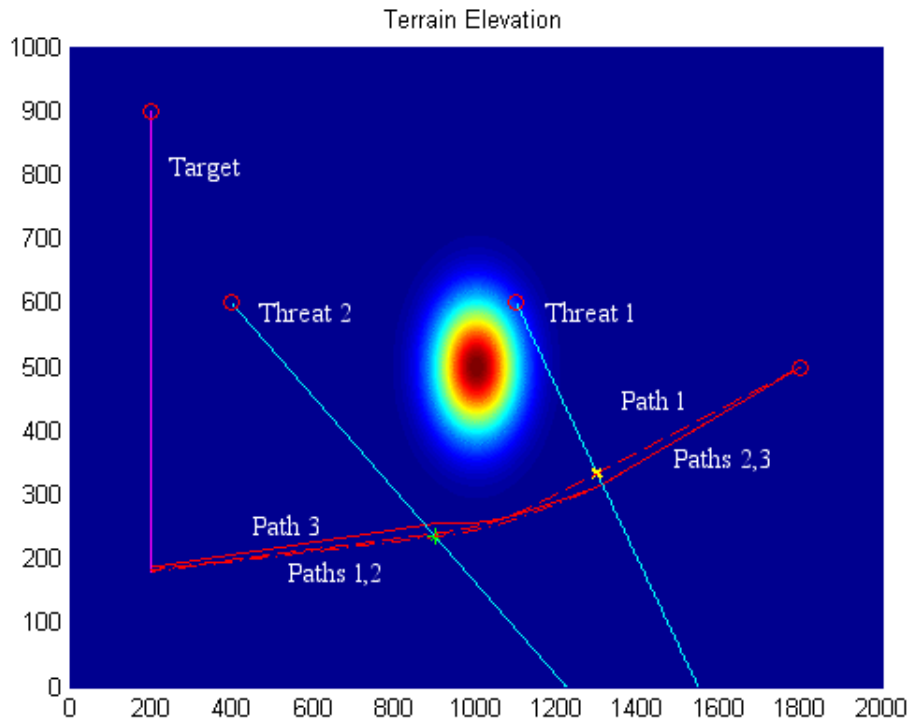


Figure 7: Paths Generated with Consideration of a Moving Target and Two Moving Threats Using Simplified Equations of Motion

In a similar manner, Figure 7 shows the results from the same scenario when the simplified equations of motion are implemented. It can be seen that the results generated using these two different sets of equations of motion are quite similar.

#### D. Pop-up Threats

The case of pop-up threats during flight was also investigated. In this case, the optimal path is in mid-flight when a stationary threat appears. A new trajectory must then be calculated. To test this, a flight through the Columbus terrain – shown in Figure 2 – was used, utilizing the constant velocity, local tangent plane equations of motion. In this case, a threat was added to the terrain as a single hill, as shown above in Figure 3, with a height of 300 feet above the level of the terrain at that point.

The results for this section can be seen in Figure 8. In this plot, the black line depicts the original trajectory found; here it goes directly through the new threat. Three different new trajectories are then shown as magenta lines. These depict the results for three different times at which the threat is found; these times are at 17.2 seconds, 29.46 seconds and at 39.79 seconds into the approximately 90 second flight. In each case, this point is marked on the plot with a red star.

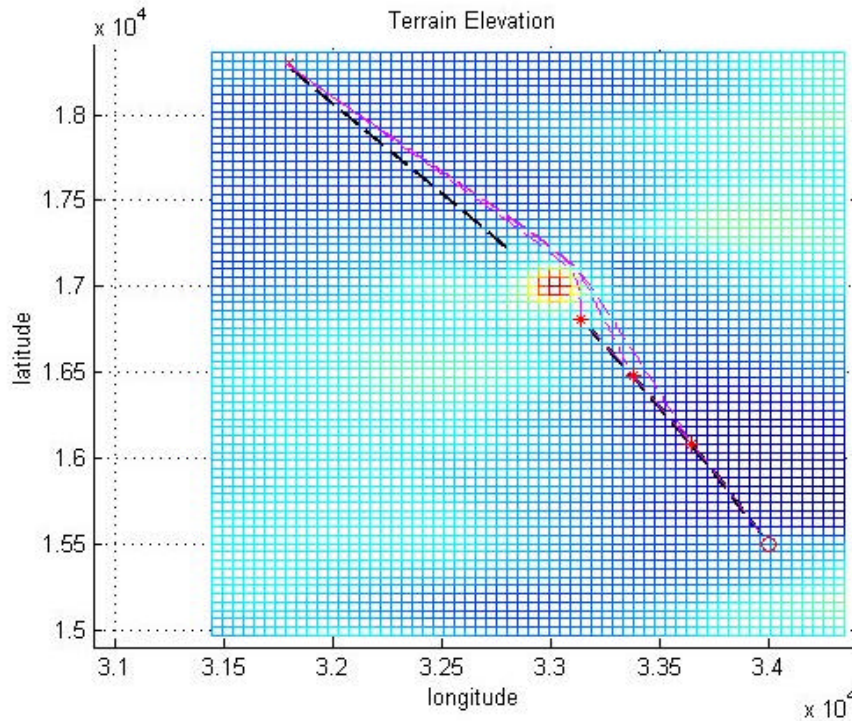


Figure 8: Trajectories Found with a Pop-up Threat Using Local Tangent Plane Equations of Motion.

#### IV. Future Research

For the time being it has been decided to continue using both the local tangent plane and simplified equations of motion. Once the trajectories can be compared using the flight simulator, the differences between the two formulations will be evaluated and a decision will be made about which formulation to use in the remainder of the project. The long-range goal is to imbed as much of the full vehicle dynamics as possible into the formulation, while maintaining a tractable solution process. Those dynamics that cannot be directly accounted for will be treated using singular perturbation methods of analysis<sup>4</sup>.

#### V. References

- (1) Kim, Eulgon. *Optimal Helicopter Trajectory Planning for Terrain Following Flight*. Thesis. Georgia Institute of Technology. 1990.
- (2) Menon, P.K., E. Kim, V.H.L. Cheng. "Optimal Trajectory Planning for Terrain Following Flight" *Journal of Guidance, Control and Dynamics*, Vol. 14, No. 4, July– August 1991, pp. 807 - 813.
- (3) United States Geological Survey. Terrain Data. <ftp://edcftp.cr.usgs.gov/pub/data/DEM/250/>
- (4) Calise, A.J., "Singular Perturbation Techniques for On-Line Optimal Flight-Path Control," *AIAA Journal of Guidance and Control*, Vol. 4, No. 4, 1981.
- (5) Bryson, A.E., Jr. and Ho, Y-C. *Applied Optimal Control*. Hemisphere Publishing Corporation, 1975.
- (6) Vanderplaats, Garret N. *Numerical Optimization Techniques for Engineering Design: With Application*. New York: McGraw-Hill Publishing Company, 1984.